International Journal of Modern Physics E
Vol. 27, No. 10 (2018) 1850086 (13 pages)

DOI: 10.1142/S0218301318500866

Possible mechanisms for production of slow target fragments

A. Abdelsalam

Mohamed EL-Nadi-High Energy Lab, Physics Department,
Faculty of Science, Cairo University, Giza, Egypt
Abdallaham@hotmail.com

M. S. El–Nagdy

Physics Department, Faculty of Science,
Helwan University, Helwan, Egypt
Physicshelwan@yahoo.com

A. M. Abdalla* and A. Saber†

Mathematics and Physics Engineering Department,
Faculty of Engineering in Shoubra,
Banha University, Cairo, Egypt
**a_abdalla65@hotmail.com*
†nasser.s2009@yahoo.com

Received 2 April 2018
Revised 12 August 2018
Accepted 12 October 2018
Published

In this paper, we investigate the possible mechanisms, which are responsible for the production of slow target fragments with energy ≤ 400 MeV that are emitted from interactions of ^{28}Si nucleus with emulsion nuclei at energy 14.6 GeV per nucleon. Angular distributions of slow fragments are compared with the corresponding results from collisions of ^{1}H, ^{3}He, ^{4}He, ^{7}Li and ^{12}C with emulsion at the energy range 2.2–3.7 A GeV. We investigate the effects of both projectile energy and mass number on the angular distributions for slow secondary charged fragments called gray and black track producing particles. The average emission angles are found to be 64° and 82° for gray and black tracks, respectively. These values are nearly constant for all compared experiments. There are two different mechanisms of gray particle production in forward and backward directions while there is a single symmetric mechanism for black particles in both directions. The temperatures are found to be 58 and 6 MeV for systems of emissions for gray and black particles, respectively. There are strong effects of target size on those mechanisms. The emission system of these particles becomes slower and shows low temperature with the increase in volume of target nucleus.

Keywords: Slow fragments; angular distribution; forward and backward emission angles.

PACS Number: 25.75.−q

*Corresponding author.

1. Introduction

Heavy ion collisions, with energy above few GeV per nucleon, are suitable conditions for studying the fine properties of nuclear matter. It gives information on the properties at high temperatures such as density, mechanism of nuclear fragmentations and initial structure of the nucleus. Much works have been performed both experimentally and theoretically for such investigations because it is more complicated due to the possible formation of new states of non-thermal equilibrium. Searching for unusual signals from formation, other intermediate nuclear states and their properties consider as very important tool for studying the new phases of the nuclear materials. These new states[1] are produced during interactions between nucleons of the interacting nuclei with sufficient collision energies. Its physical properties play the major role and control the characteristics of secondary particles. Studying the behavior of interactions helps to get some important information about the dynamics of the collisions. In experiments, it is impossible to measure all parameters that describe the kinematic of the interactions but it can be calculated from theoretical models, which are assumed according to the predictions of different assumptions. One of the experimental parameters that is used to describe the nucleus–nucleus collisions is the angular distributions of fission fragments.[2] This parameter is an important probe and it can describe the possible mechanisms of fragmentation for both projectile, target nuclei, and investigate the particular flow of the observables and production of secondary particles. In addition, it describes the formation and decay of some intermediate stages of interacting nuclei. The main aim of this work is studying experimental behavior of the angular distributions of slow and heavy fission fragments produced from interactions of silicon ions with composite target of emulsion nuclei at energy 14.6 GeV per nucleon. In previous work[2] analysis of the experimental results concluded that the angular distributions of secondary fragments are sensitive to entrance channel parameters as well as the statistical aspects of intermediate system as it evolves in time. In this work, the obtained data will be studied in terms of the prediction of the statistical model[3,4] to investigate the mechanism responsible for secondary particle production.

2. Statistical Model

Statistical model defines a mathematical relationship between collections of variables, each variable being a vector of readings of a specific trait on the samples in an experiment. It explains in what way a variable depends on other variables in the study. Statistical model gives mathematical formulation, which embodies a set of assumptions concerning the generation of some sample data. This formulation correlates some of expected and other random variables. The assumptions embodied by statistical model generate a set of probability distributions some of which may be adequate to the experiment results than other models. The distribution of emitted secondary particles as a function of the emission angle θ, which are measured from direction of incident projectile, is one of the important experimental parameters that describes the temperature and mechanism responsible for particle emission. To study this mechanism, we will use statistical model for Maxwell distribution[3] for secondary emitted particle and their multiplicities according to their momentum as (let $c = 1$)

$$\frac{d^2N}{dPd\mu} \propto P^2 \exp\left\{-\frac{(P^2 - 2M\bar{\beta}_{\|}P_{\mu})}{P_o^2}\right\}, \tag{1}$$

where $\beta_{\|}$, is the longitudinal velocity of the particle-emitting system. $\mu = \cos\theta$, where θ is the laboratory angle between the momentum of the fragment of mass M and the momentum of the initial projectile, and $P_o = \sqrt{2ME_o}$, where E_o is the characteristic energy per particle in the hypothetical moving system. Equation (1) would be modified when it is expressed in terms of range of the tracks and angle of emissions or μ, where the two quantities are measured in the experiment. Good approximation is applied for particle production according to the angle of emission into forward and backward emissions with predicted ratio F/B, and rational velocity χ_o, where

$$\chi_o = \frac{\beta_{\|}}{\beta_o} = \frac{\bar{\beta}_{\|}}{\bar{\beta}_o} \tag{2}$$

which is the ratio of the longitudinal velocity of the center of mass, $\beta_{\|}$, to the characteristic spectral velocity β_o, of the fragmenting system. When the angular distributions are measured without regard to fragment velocity, $dN/d\mu$ becomes a function of the single fitting parameter χ_o only where

$$\frac{dN}{d\mu} \approx \exp\left(\frac{4}{\sqrt{\pi}}\chi_o\mu\right), \tag{3a}$$

$$\frac{F}{B} \approx \exp\left(\frac{4}{\sqrt{\pi}}\chi_o\right). \tag{3b}$$

Hence,

$$\frac{dN}{d\mu} \approx \left(\frac{F}{B}\right)^{\mu}, \tag{3c}$$

$$\frac{dN}{d\theta} \approx \sin\theta\left(\frac{F}{B}\right)^{\cos\theta}. \tag{3d}$$

The values of F/B were obtained in the experiment and Eq. (3a) was a suitable approximation of the exact expression $dN/d\mu$.

3. Experimental Details

The data, which are used in this work, are the experimental results of nucleus–nucleus collisions using the nuclear photo-emulsion detector. The details of these experiments and primary results are published in Refs. 5–7. Nuclear emulsion plates are photographic plates with a particularly thick emulsion layer and with uniform grain size. Emulsion plates record the tracks of charged particles passing through. Charged particle in emulsion makes many inelastic collisions with atoms such as silver halides. Atoms along this path lost electrons and became ionized forming a latent image. After chemical development, they formed image could be seen as collection of bulbs and specified by grain density g, which characterizes the charge and velocity of the moving particle. The sensitivity of the used emulsion of FUJI type for single relativistic charged particle is $g_o = 30$ grains per $100\,\mu$m of track length. It exposed to ^{28}Si beam with energy 14.6 A GeV at Brookhaven National Laboratory (BNL) Alternating Gradient Synchrotron (AGS). The identification of any secondary charged particles is completed by counting the grain density g and so the normalized grain density g^*, where $g^* = g/g_o$. According to the magnitudes of g^* of the tracks, the secondary charged particles are identified and classified into three groups of tracks. First are particles with tracks appearing as slower tracks with $g^* \leq 1.4$ corresponding to relativistic particles with velocity $\beta = v/c \geq 0.7$. Most of these tracks are due to mesons of energy above 50 MeV and small fraction of fast protons with energy above 400 MeV. The second group of tracks consists of gray tracks producing particles or gray particles (g-particles) with $1.4 < g^* \leq 10$ and velocity with $0.3 < \beta < 0.7$. These tracks are recoil protons with energy 26 up to 400 MeV and contaminated deuterons, tritons and helium nuclei. The last group of tracks is called black track producing particles or black particles (b-particles). These particles take $g^* \geq 10$ and velocity of $\beta \leq 0.3$. It represents slow protons of energy below 26 MeV and deuteron, alpha particles and heavy fragments. The gray tracks and the black tracks are known as tracks of the heavily ionizing particles with the value of the velocity $\beta < 0.7$. The heavily ionizing particles multiplicity is denoted by N_h.

In this experiment, the target is composite nucleus. The inelastic interactions are classified into three groups, first is the interaction of ^{28}Si with hydrogen nucleus, H. The second group includes interactions with light emulsion component carbon, nitrogen, and oxygen, CNO. The third group includes interactions with heavy emulsion components silver and bromine AgBr. The separation of the interactions is based on the multiplicity N_h. Experimental tools for separation of interactions are explained in detail in Refs. 8 and 9. Interactions of $N_h \leq 1$ are with hydrogen nuclei while with CNO are those of $2 \leq N_h \leq 7$. The third interactions with heavy target group AgBr are of $N_h \geq 8$ with contaminated in range $N_h \leq 7$. The overlapped region is small to change the results for interactions with CNO group.

4. Experimental Results

4.1. *Angular distribution of gray particles*

Initially, we study different mechanisms responsible for gray particle (g-particle) production from interactions of different projectiles with compound target nuclei of emulsion. Figure 1 shows the experimental results for angular distributions of

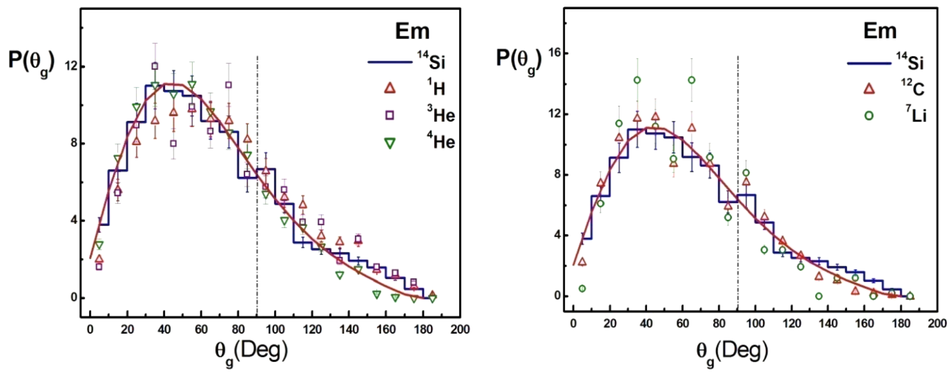

(a) (b)

Fig. 1. The angular distribution of gray particles emitted in ^{28}Si-Em interactions at 14.6 A GeV compared with corresponding ^{1}H, ^{3}He and ^{4}He in (a) and with ^{12}C and ^{7}Li in (b). Smooth curve represents the corresponding prediction of the statistical model.

g-particles emitted from ^{28}Si-Em at 14.6 A GeV (histogram) compared with the corresponding distributions at energy 3.7 A GeV for ^{1}H,[4] ^{3}He,[10] ^{4}He[4] in (a), ^{7}Li and ^{12}C[11] in (b). Generally, all distributions are in the same trend irrespective of both projectile energy and mass number. These results explain that the effect of projectile energy, in this range, is sufficient to make each projectile and target nuclei in a state of full destruction with limited fragmentation processes. The effect of projectile mass number on angles of the production system of g-particles is absent because such mechanism is constant and independent on a number of participant projectile nucleons.

The angular distributions of g-particles for all projectiles can be described by Rayleigh distribution that is often observed when the overall magnitude of a vector is related to the directional components. It comes from in-isotropic medium with two trends observed at separation angle of 90°. The first is the forward emission at $\theta \leq 90°$ and the second is the backward emission at $\theta > 90°$. In the forward emission, experimental data is represented by Rayleigh distribution, which is Gaussian-like distribution, with two symmetric sides. It can describe particle production due to homogenous source around the average value of the emission angle. The forward emission mechanism of g-particles production is explained in terms of the effect of momentum of projectile nucleons on target nucleus to be fragment in the forward angles. The second mechanism is the backward emission which is represented by exponential decay curve where particles production gradually decreases with increasing angle of emission. Its behavior is explained as cooling curve of target nucleus and backward emission is due to evaporated target fragments.[19] These two trends are observed for the all used projectiles. In Fig. 1, the smooth line represents the predictions for statistical model according to the fitting shape from Eq. (3d) when applied for g-particles. The predicted rational velocity χ_o^g, is calculated from the statistical model by using the following equation

$$\chi_o^g = \frac{\beta_{\|g}}{\beta_\circ} = \cos(\langle\theta_g\rangle). \tag{4}$$

It is noticed that within experimental errors the distribution predicted by statistical model is in good agreement with experimental data. The mean value of the emission angles $\langle\theta_g\rangle$ for gray particles is defined as the medium angle, i.e., the angle at which half of the number of the specified particles is emitted. It is compared with the different projectiles in the range of energy 3.7–14.6 A GeV and magnitudes of the parameter χ_o^g and $\beta_{\|g}$ are given in Table 1. The comparison shows that these parameters are nearly constant and independent on projectile mass number which reflects the constancy of the mechanisms which are responsible for emission of this particles. From Table 1 and Fig. 1 it is noticed that, the constancy in the values of $\langle\theta_g\rangle \sim 64^\circ$, independent of the variation of the projectile mass number as well as incident energy. The rational velocity for the system of gray particle emission χ_o^g is nearly equal to 0.5 for all interactions. The emitting system of the g-particles is fast with typical longitudinal velocities $\beta_{//}^g \approx 0.13$–$0.20$. The anisotropic ratio $(F/B)_g$ is the ratio of the number of forward fragments of g-particles to that emitted in the backward fragment for different projectiles are given in Table 1. These ratios appear constant and range between 2.5 to 3.9. It proves that all predictions of statistical models for all given projectiles are similar and controlled by two fixed mechanisms for g-particle production. In Ref. 10, similar conclusions were observed for oxygen and sulfur at 200 A GeV.

In this section, we explain the effect of target size on the angular distribution of g-particles. In Sec. 3 and in our previous work[20,21] we stated that the emulsion is compound target and collisions are classified into three main groups according to multiplicity of heavily ionizing the secondary charged particle N_h. These particles are pure target fragments and can be considered as experimental parameters, which describe the degree of overlapping of projectile and target nuclei. First group

Table 1. The average values of the emission angles of the gray particles $\langle\theta g\rangle$ in different interactions with emulsion at energy 3.7–14.6 A GeV, in addition $^{28}Si + CNO$ and $^{28}Si + AgBr$. The rational velocity of the system χ_o^g, ratio $(F/B)_g$ and longitudinal velocity $\beta_{\|g}$ based on statistical model.

Projectile	$\langle\theta_g^\circ\rangle$	χ_o^g	$(F/B)_g$	$\beta_{\|g}$	Ref.
^{1}H	67.80 ± 1.2	0.59	3.80 ± 0.20	0.20	4
^{4}He	62.80 ± 3.1	0.48	3.00 ± 0.30	0.17	4
^{6}Li	64.90 ± 2.2	0.47	2.90 ± 0.20	0.16	12
^{7}Li	63.50 ± 2.0	0.45	3.82 ± 0.20	0.16	11 and 13
^{12}C	64.00 ± 1.9	0.55	3.51 ± 0.20	0.19	4
^{22}Ne	63.70 ± 1.6	0.55	3.50 ± 0.12	0.19	13
^{28}Si	63.30 ± 1.4	0.55	3.52 ± 0.16	0.19	4, 14–16
^{28}Si	64.76 ± 2.1	0.49	3.05 ± 0.27	0.17	Present work
$^{28}Si + CNO$	62.44 ± 5.2	0.46	2.84 ± 0.24	0.16	Present work
$^{28}Si + AgBr$	65.56 ± 3.5	0.41	2.54 ± 0.25	0.14	Present work

with multiplicity $N_h \leq 1$ includes interactions with hydrogen and low statistics are excluded from this consideration. Second group includes the interactions with light emulsion components CNO, where $2 \leq N_h \leq 7$ and are considered as gentle interactions. Third group includes interactions of ^{28}Si with heavy emulsion nuclei AgBr. It is considered as hard interactions and characterized by $N_h \geq 8$. Figure 2 shows the angular distributions of g-particles emitted from interactions of ^{28}Si with CNO compared with ^{1}H, ^{3}He and ^{4}He in Fig. 2(a) and ^{12}C and ^{7}Li in Fig. 2(b). Figure 3 shows the corresponding distributions for collisions with AgBr. The figures show that the angular distributions for both two-target components are different from each other. For gentle interactions, most probable angles are in forward hemisphere and minimum probability for angles in backward direction because the effect of projectile momentum in forward direction strongly appears for interactions with light target nuclei. In hard interactions, fluctuation is limited in the forward direction while most fluctuations are observed in the backward hemisphere which gradually decrease with angles to reach minimum multiplicity in opposite direction ($\theta = 180°$). This is noticed in ratio $(F/B)_g$ in Table 1. For gentle interactions, its value is 2.84 ± 0.24 while it decreases to 2.54 ± 0.25 for hard interactions. In addition, the average angle of emission for gentle interactions is $62.44° \pm 5.18$ and it increases to $65.56° \pm 3.51$ for hard interactions. The rational parameter $\chi^g_\circ$ decreases with target mass number, i.e., the system responsible for emission of g-particles becomes slower. This is expected due to the effect of target size on the velocity of the system responsible for particle production. This becomes sufficient for projectile nucleons to lose its momentum up to be emitted as recoil fragments in wide range of angles. This results are noticed for all compared and different projectiles, which proved that there are two different mechanisms responsible for

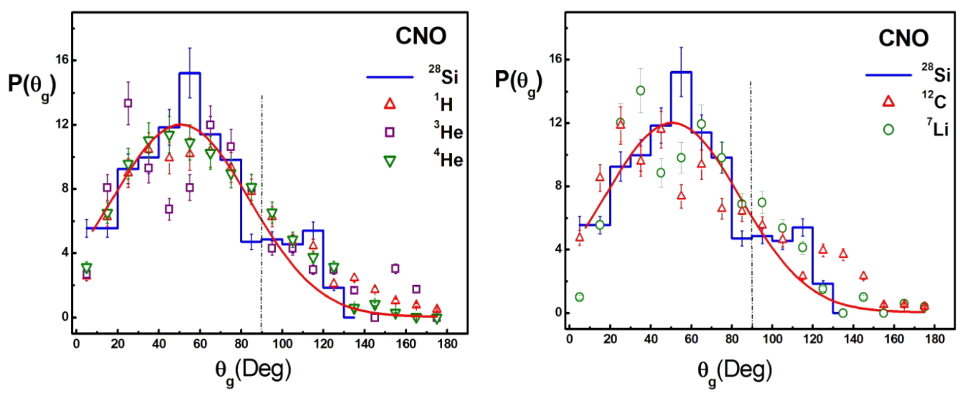

(a) (b)

Fig. 2. The angular distribution of gray particle emitted ^{28}Si interactions at 14.6 A GeV with light emulsion component CNO compared with the corresponding distribution for ^{1}H, ^{3}He and ^{4}He in (a) and with ^{12}C and ^{7}Li in (b). Smooth curve represents the corresponding prediction of the statistical model using Gaussian-fitting shape.

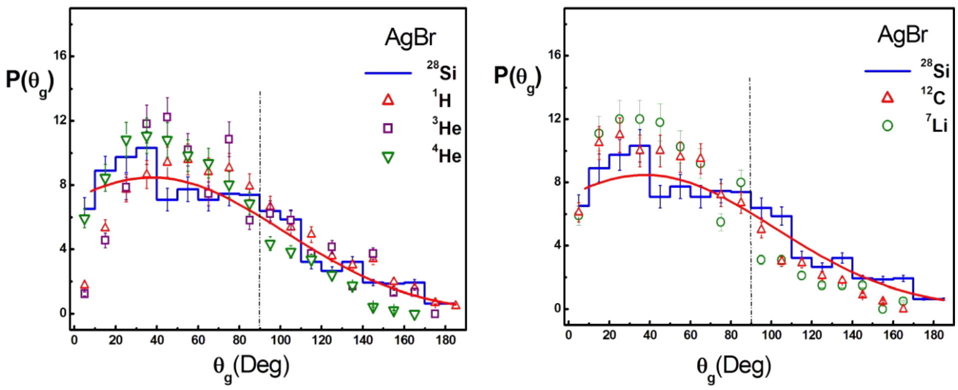

(a) (b)

Fig. 3. The angular distribution of gray particle emitted ^{28}Si interactions at 14.6 A GeV with heavy emulsion component AgBr compared with the corresponding distribution for ^{1}H, ^{3}He and ^{4}He in (a) and with ^{12}C and ^{7}Li in (b). Smooth curve represents the corresponding prediction of the statistical model using Gaussian-fitting shape.

g-particles production one for forward emission and other for backward direction. The effect of the target size is observed on the two production mechanisms.

4.2. *Angular distribution of black particles*

Secondly, we study the angular distributions and properties of the mechanism responsible for the production of slow particles, which appear as black tracks in emulsion experiments. These particles play an important role in describing the nature of the interactions between projectile and target nuclei. Figure 4 shows the

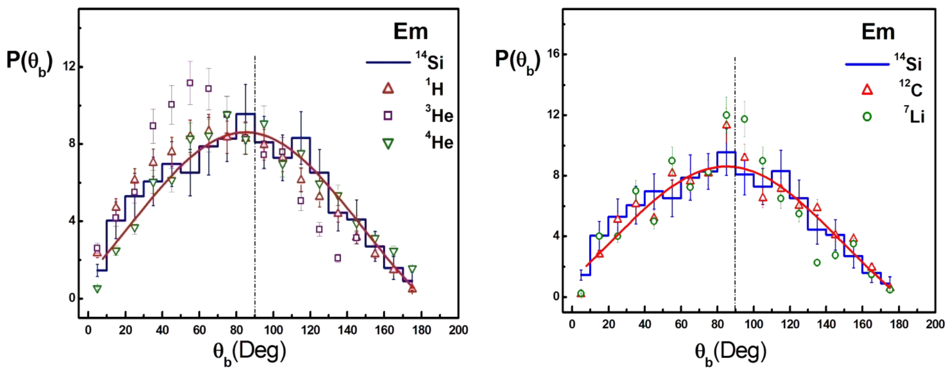

(a) (b)

Fig. 4. The angular distribution of black particles emitted in ^{28}Si-Em interactions at 14.6 A GeV compared with corresponding ^{1}H, ^{3}He and ^{4}He in (a) and with ^{12}C and ^{7}Li in (b). Smooth curve represents the corresponding prediction of the statistical model.

Table 2. The average values of the emission angles of the black particles $\langle\theta_b\rangle$ in different interactions at energy 2.2–14.6 A GeV, in addition to the rational $\chi_\circ^b$ velocity of the system, the ratio $(F/B)_b$ and longitudinal velocity $\beta_{\|_b}$ of black particle emission, on the basis of statistical model.

Projectile	$\langle\theta_b\rangle$	χ_o^b	$(F/B)_b$	$\beta_{\|_b}$	Ref.
^{1}H	85.3 ± 1.9	0.11	1.28 ± 0.1	0.013	4
^{4}He	83.0 ± 3.8	0.13	1.35 ± 0.1	0.015	4
^{6}Li	82.2 ± 2.6	0.12	1.30 ± 0.2	0.018	12
^{7}Li	81.3 ± 2.3	0.11	1.28 ± 0.1	0.013	11 and 13
^{12}C	79.5 ± 2.4	0.11	1.27 ± 0.1	0.013	4
^{28}Si	83.3 ± 1.2	0.20	1.59 ± 0.1	0.023	14, 18, 19
^{28}Si	83.5 ± 1.9	0.11	1.26 ± 0.1	0.013	Present work
^{28}Si + CNO	79.9 ± 3.7	0.17	1.48 ± 0.1	0.019	Present work
^{28}Si + AgBr	84.9 ± 2.2	0.09	1.22 ± 0.1	0.010	Present work

angular distributions of the b-particles compared to those recorded for ^{1}H, ^{3}He and ^{4}He in (a) and for ^{7}Li and ^{12}C in (b). The average values of the emission angle for different interactions are given in Table 2. Within experimental errors, the angular distributions for using projectiles are in the same trend and the mean emission angles approximately take fixed value. It concludes that the mechanism responsible for emission of b-particles is independent of projectile size and its energy because these particles are pure target fragments. It is noted that the spectrum seems to be symmetric around the peak position, which is near the mean value $\langle\theta_b\rangle$.

The feature of this spectrum implies that the emission of b-particles, in forward and backward hemispheres, tends to be symmetric in both directions where the maximum particle multiplicity approaches the region of $\theta_{\rm lab} \sim 90°$. The similarity for particle emission is different from that observed for g-particles. It proves that, for both directions, there is a single mechanism responsible for b-particle production. This mechanism is independent of projectile mass number and interaction energy. It is characterized by isotropic thermal excitation of target nucleus and the system temperature is uniformly distributed over most target nucleons. In the last stage of collision, target nucleus begins to cool by the emission of heavy fragments along the wide range of angles, which are independent of the direction of incident projectile. The fragments are massive particles with minimum energy and residual target nucleus.

Angular distribution of b-particles emitted from ^{28}Si–Em interactions at energy 14.6 A GeV compared with the corresponding prediction of statistical model (smooth line) are shown in Fig. 4. The predicted distribution by the model shows good agreement with experimental results. The model predicts the rational velocity $\chi_\circ^b$ and longitudinal velocity $\beta_{\|_b}$ where their values are given in Table 2. The magnitude of $\beta_\circ^b$ is taken to be ∼0.115 from Ref. 4. We can conclude that the constancy in the values of $\langle\theta_b\rangle \sim 83°$ is independent of the variation of projectile mass number as well as projectile energy. The rational velocity $\chi_\circ^b$ tends to be ∼0.13 for the system of black particles. The ratio $(F/B)_b$ for different projectiles is more concise in small range 1.2–1.6 which supports the prediction of the fixed mechanism of b-particle production and different from that for the gray system. The emitting system of the b-particles is slow and has a typical longitudinal velocities $\beta^b_{//}$ whose range is $\beta^b_{//} \sim 0.010{-}0.023$. The temperature of the emitting system can be calculated using $T = 1/2M\beta_\circ^2$ where M is the nucleon mass. Its value for black particles is found to be 6 MeV per nucleon. It is approximately equal to the binding energy per nucleon at the normal state of the nucleus. The corresponding temperature for the system responsible for g-particle production is calculated by using the magnitude of

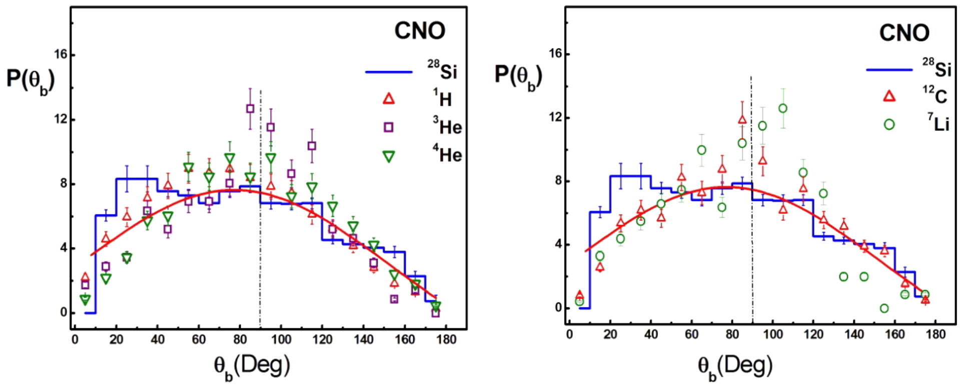

(a) (b)

Fig. 5. The angular distribution of black particle emitted ^{28}Si interactions at 14.6 A GeV with light emulsion component CNO compared with the corresponding distribution for ^{1}H, ^{3}He and ^{4}He in (a) and with ^{12}C and ^{7}Li in (b). Smooth curve represents the corresponding prediction of the statistical model using Gaussian-fitting shape.

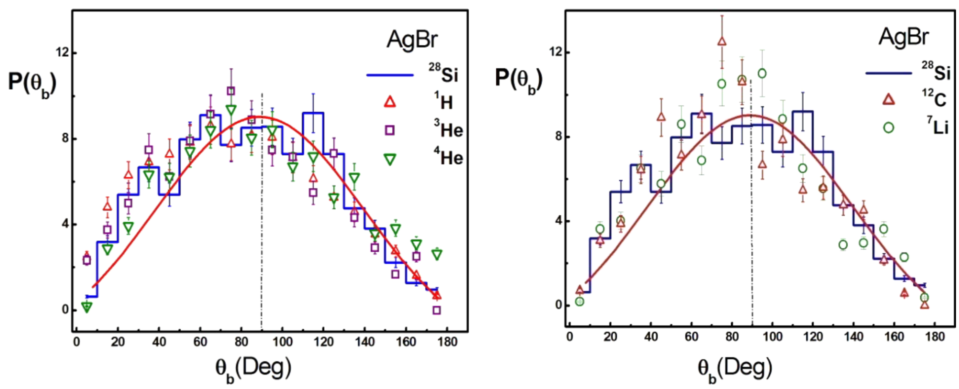

(a) (b)

Fig. 6. The angular distribution of black particle emitted ^{28}Si interactions at 14.6 A GeV with light emulsion component AgBr compared with the corresponding distribution for ^{1}H, ^{3}He and ^{4}He in (a) and with ^{12}C and ^{7}Li in (b). Smooth curve represents the corresponding prediction of the statistical model using Gaussian-fitting shape.

$\beta^g_\circ \sim 0.35$ (Ref. 4). The value is found to be 58 MeV per nucleon, which is sufficient for nucleon to make a cascade of secondary interactions before escaping from hot size of interactions.

The final point of interest is the effect of target size on angular distributions of b-particles. The effects for both two-target components are shown in Fig. 5 for gentle interaction with CNO and Fig. 6 for hard interaction with AgBr. The experimental and predicted parameters are given in Table 2.

It is noticed that there is clear effect of target size on mechanism responsible for black particle productions. For gentle interactions, the emission of evaporated b-particles begins from angles 20° and most probabilities are nearly constant in forward direction up to 90° while in backward directions, the probability begins, fast decreasing with angles. This could be explained by assuming that for small target size (CNO), there is strong effect of projectile momentum on the angles of the emission of black fragments. This effect disappears for hard interactions and distributions show clear symmetric around middle angle. The mean values of emission angles are about 85° and 80° for hard and gentle interactions, respectively. These values proved that the angular distributions are more symmetric for hard interactions and slightly deviate for gentle interactions. The ratio $(F/B)_b$ and rational parameter $\chi^b_\circ$ increase from 1.22 ± 0.07 and 0.09 for hard interactions to 1.48 ± 0.08 and 0.17 for gentle interactions, respectively. It proves that the system of emission for black particles becomes slower and shows low temperature with increasing mass number of the interacting target nucleus.

5. Conclusions

(1) The angular distributions of each of gray and black particles are independent of each projectile mass number and projectile energy.

(2) The angular distribution for g-particles indicates two mechanisms for particle production: one for forward particle which takes homogenous Gaussian distribution due to the effect of projectile momentum and the second in backward emissions due to recoil protons from both projectile and target nucleons.

(3) The angular distributions of gray and black particles, which emitted from ^{28}Si-Em interactions at energy 14.6 A GeV, are well described by the statistical model.

(4) The experimental parameters such as mean values of the emission angles for g-particles are $\langle\theta_g\rangle \sim 64°$ and for b-particles are $\langle\theta_b\rangle \sim 83°$. These values are nearly constant for the corresponding collisions using different mass number of the projectiles in the range of collisions energies 2.2–14.6 A GeV.

(5) The predicted rational velocity by statistical model χ_o which describes the system that is responsible for emission of the secondary particles is nearly equal to 0.5 for g-particles and tends to be ∼0.13 for b-particles.

(6) The velocity of the emitting system is described by the parameter $\beta_{//,}$ where the emitting system for g-particles is fast and with typical longitudinal

velocities $\beta^{g}_{//} \sim 0.13-0.20$ while it is slow for emission of *b*-particle in the range $\beta^{b}_{//} \sim 0.008-0.019$.

(7) The anisotropic ratio F/B is found to be 2–3 for the system that is responsible for *g*-particle productions while it is 1.2–1.6 for the system of *b*-particle production.

(8) The temperatures of the system, which is responsible for emission of secondary slow fragments, are found to be 58 MeV for *g*-particle productions while 6 MeV for *b*-particles.

(9) The angular distributions for both gray and black particles depend on the size of the target nucleus. Most of the emission angles for *g*-particles are mainly in forward angles for small target nuclei CNO, while it is in symmetry distributions between forward and backward hemispheres for heavy target AgBr.

(10) The systems, which are responsible for gray and black particle productions, become slower and show low temperature with increasing target mass number.

Acknowledgment

The authors would like to thank P.L. Jain for supplements of the irradiated emulsion plates.

References

1. S. K. Karn, R. S. Kaashal and Y. K. Mathur, *Z. Phys. C* **72** (1996) 297.
2. A. Abdelsalam, M. Šumbera and S. Vokál, *JINR* Report (Dubna) El-82–509 (1982).
3. H. H. Hackmann, H. J. Crawford, D. E. Greiner, P. J. Lindstrom and W. Wilson Lamce, *Phys. Rev. C* **17** (1978) 1651.
4. A. Abdelsalam, *Phys. Scr.* **47** (1993) 124.
5. M. El-Nadi, M. S. El-Nagdy, N. Ali-Mossa, A. Abdelsalam, A. M. Abdalla and A. A. Hamed, *J. Phys. G*, *Nucl. Phys.* **25** (1999) 1169.
6. M. El-Nadi *et al.*, *Eur. Phys. J. A*, *Hadrons Nuclei* **10** (2001) 177.
7. M. El-Nadi *et al.*, *J. Phys. G*, *Nucl. Part. Phys.* **28** (2002) 1251.
8. J. R. Florian *et al.* Report submitted to the meeting of division of particles and fields, Berkely, California (1973).
9. A. Abdelsalam, JINR Report (Dubna) El-81–623 (1981).
10. A. Abdelsalam, M. S. El-Nagdy, N. Rashed, B. M. Badawy and E. El-Falaky, *J. Nucl. Radiat. Phys.* **2** (2007) 49.

AQ: Kindly provide page number.

11. M. El-Nadi, A. Abdelsalam, M. M. Sherif, N. Ali-Moussa, M. S. El-Nagdy, *IL Nuovo Cimento* **107** (1994).
12. M. I. Adamovich *et al.*, LUND Report LUIP 8906 (1989).
13. M. M. Sherif, *Il Nuovo Cimento* **109A** (1996) 1135.
14. M. El-Nadi, A. Abdelsalam and N. Ali-Moussa, *Int. J. Mod. Phys. E.* **3** (1994) 811.
15. Z. Dong-Hai and LI. Hui-Ling, *Chin. Phys. C* **33** (2009) 345.
16. A. Abdelsalam, B. M. Badawy and E. El-Falaky, *Can. J. Phys.* **85** (2007) 837.
17. A. Abdelsalam, M. S. El-Nagdy, A. M. Abdalla and A. Saber, *Int. J. Mod. Phys. E* **24** (2015) 1550084.
18. M. El-Nadi, A. Abdelsalam, N. Ali-Moussa, Z. Abou-Moussa, Kh. Abdel-Waged, W. Osman and Badawy, *IL Nuovo Cimento A* **111** (1998) 1243.

19. M. El-Nadi, A. Abdelsalam and N. Ali-Moussa, *Radiat. Phys. Chem.* **47** (1996) 681.
20. M. S. El-Nagdy, A. Abdelsalam, B. M. Badawy, P. I. Zarubin, A. M. Abdalla and A. Saber, *Chin. Phys. Lett.* **35** (2018) 032501.
21. M. S. El-Nagdy, A. Abdelsalam, B. M. Badawy, P. I. Zarubin, A. M. Abdalla, M. Nabil Yasin, A. Saber, M. M. Mohamed and M. M. Ahmed, *J. Phys. Commun.* **2** (2018) 035010.